Gutteridge, S., Reddy, G. S., & Lorimer, G. H. (1989) *Biochem. J. 260*, 711-716.
Hemmingsen, S. M., Woolford, C., van der Vies, S. M., Tilly, K., Dennis, D. T., Georgeopoulos, C., Hendrix, R. W., & Ellis, R. J. (1988) *Nature 333*, 330-334.
Hendrix, R. W. (1979) *J. Mol. Biol. 129*, 375-392.
Hoess, A., Arthur, A. K., Wanner, G., & Fanning, E. (1988) *Bio/Technology 6*, 1214-1217.
Hohn, T., Hohn, B., Engel, A., Wurtz, M., & Smith, P. R. (1979) *J. Mol. Biol. 129*, 359-373.
Ishihama, A., Ikeuchi, T., & Yura, T. (1976a) *J. Biochem. (Tokyo) 79*, 917-925.
Ishihama, A., Ikeuchi, T., Matsumoto, A., & Yamamoto, S. (1976b) *J. Biochem. (Tokyo) 79*, 927-936.
Janolino, V. G., Sliwkowski, M. X., Swaisgood, H. E., & Horton, H. R. (1978) *Arch. Biochem. Biophys. 191*, 269-277.
Kusukawa, N., Yura, T., Ueguchi, C., Akiyama, Y., & Ito, K. (1989) *EMBO J. 8*, 3517-3522.
Lill, R., Cunningham, K., Brundage, L. A., Ito, K., Oliver, D., & Wickner, W. (1989) *EMBO J. 8*, 961-966.
Lubben, T. H., Donaldson, G. K., Viitanen, P. V., & Gatenby, A. A. (1989) *Plant Cell 1*, 1223-1230.
McMullin, T. W., & Hallberg, R. L. (1988) *Mol. Cell. Biol. 8*, 371-380.
Miller, R. P., & Farley, R. A. (1990) *Biochemistry 29*, 1524-1532.
Ostermann, J., Horwich, A. L., Neupert, W., & Hartl, F.-U. (1989) *Nature 341*, 125-130.
Picketts, D. J., Mayanil, C. S. K., & Gupta, R. S. (1989) *J. Biol. Chem. 264*, 12001-12008.
Pierce, J., & Gutteridge, S. (1986) *Appl. Environ. Microbiol. 49*, 1094-1100.
Pierce, J., & Reddy, G. S. (1986) *Arch. Biochem. Biophys. 245*, 483-493.
Roy, H., Bloom, M., Milos, P., & Monroe, M. (1982) *J. Cell Biol. 94*, 20-27.
Schloss, J. V., Phares, E. F., Long, M. V., Norton, I. L., Stringer, C. D., & Harman, F. C. (1982) *Methods Enzymol. 90*, 522-528.
Sinha, N. K., & Light, A. (1975) *J. Biol. Chem. 250*, 8624-8629.
Suelter, C. H. (1974) *Met. Ions Biol. Syst. 3*, 201-251.
Tilly, K., & Georgeopoulos, C. P. (1982) *J. Bacteriol. 149*, 1082-1088.
Van Dyk, T. K., Gatenby, A. A., & LaRossa, R. A. (1989) *Nature 342*, 451-453.
Zweig, M., & Cummings, D. J. (1973) *J. Mol. Biol. 80*, 505-518.

# Identification and Localization of Bound Internal Water in the Solution Structure of Interleukin 1$\beta$ by Heteronuclear Three-Dimensional $^1$H Rotating-Frame Overhauser $^{15}$N-$^1$H Multiple Quantum Coherence NMR Spectroscopy†

G. Marius Clore,*,‡ Ad Bax,‡ Paul T. Wingfield,§ and Angela M. Gronenborn*,‡
*Laboratory of Chemical Physics, Building 2, National Institute of Diabetes and Digestive and Kidney Diseases, and Protein Expression Laboratory, Building 6B, National Institutes of Health, Bethesda, Maryland 20892*
*Received April 6, 1990*

ABSTRACT: The presence and location of bound internal water molecules in the solution structure of interleukin 1$\beta$ have been investigated by means of three-dimensional $^1$H rotating-frame Overhauser $^1$H-$^{15}$N multiple quantum coherence spectroscopy (ROESY-HMQC). In this experiment through-space rotating-frame Overhauser (ROE) interactions between NH protons and bound water separated by $\leq$3.5 Å are clearly distinguished from chemical exchange effects, as the cross-peaks for these two processes are of opposite sign. The identification of ROEs between NH protons and water is rendered simple by spreading out the spectrum into a third dimension according to the $^{15}$N chemical shift of the directly bonded nitrogen atoms. By this means, the problems that prevent, in all but a very few limited cases, the interpretation, identification, and assignment of ROE peaks between NH protons and water in a 2D $^1$H-$^1$H ROESY spectrum of a large protein such as interleukin 1$\beta$, namely, extensive NH chemical shift degeneracy and ROE peaks obscured by much stronger chemical exchange peaks, are completely circumvented. We demonstrate the existence of 15 NH protons that are close to bound water molecules. From an examination of the crystal structure of interleukin 1$\beta$ [Finzel, B. C., Clancy, L. L., Holland, D. R., Muchmore, S. W., Watenpaugh, K. D., & Einspahr, H. M. (1989) *J. Mol. Biol. 209*, 779-791], the results can be attributed to 11 water molecules that are involved in interactions bridging hydrogen-bonding interactions with backbone amide and carbonyl groups which stabilize the 3-fold pseudosymmetric topology of interleukin 1$\beta$ and thus constitute an integral part of the protein structure in solution.

Bound water molecules are invariably present in high-resolution X-ray structures where they may be found either within the interior of the protein or on the surface (Deisenhofer & Steigemann, 1975; Blundell & James, 1976; Finney, 1979; James & Sielecki, 1983; Edsall & McKenzie, 1983; Baker & Hubbard, 1984; Teeter, 1984; Wlodawer et al., 1987). Internal water molecules often play a role in stabilizing the protein structure through bridging hydrogen-bonding interactions and additionally may be involved in catalysis (Bode & Schwager,

† This work was supported by the Intramural AIDS Directed Anti-Viral Program of the Office of the Director of the National Institutes of Health.
‡ Laboratory of Chemical Physics.
§ Protein Expression Laboratory.

1975; Branden et al., 1975; Rees et al., 1983). Ordered surface waters, on the other hand, tend to be clustered around polar groups (Carter et al., 1974; Rose, 1978; Brünger et al., 1985). Evidence for water molecules bound to proteins in solution has come from a number of sources, which include the demonstration of a layer of hydration through magnetic relaxation experiments (Koenig et al., 1978; Halle et al., 1981; Shirley & Bryant, 1982) and the measurement of bound water exchange with $^{18}O$ tracer techniques (Tüchsen et al., 1987). It is only very recently, however, that bound internal water has been directly observed in a small protein in solution, namely, bovine pancreatic trypsin inhibitor, by means of 2D[1] rotating-frame Overhauser (ROESY) experiments (Otting & Wüthrich, 1989). The rational behind the ROESY experiment lies in its ability to distinguish interactions between protein protons and water arising from through-space (<4 Å) nuclear Overhauser effects and chemical exchange, as these two processes give rise to cross-peaks of opposite sign (Bothner-By et al., 1984; Bax & Davis, 1985; Davis & Bax, 1985). This contrasts to conventional 2D NOESY experiments in the laboratory frame where NOE and chemical exchange peaks are of the same sign and hence indistinguishable (Jeener et al., 1979). Unfortunately, the application of 2D methods to the identification of bound water molecules is very limited, because all such interactions give rise to cross-peaks on a single trace of the 2D spectrum, parallel to the $F_2$ axis at the $F_1$ frequency of the $H_2O$ resonance. This particular trace often shows severe base-line distortion caused by the intense $H_2O$ resonance. Moreover, extensive resonance overlap often occurs on this trace due to the multitude of exchange, ROE, and ROE–exchange (vide infra) interactions. Consequently, many of the ROEs between NH protons and water may be obscured by the presence of much stronger chemical exchange peaks located at the same frequency, effectively wiping out any intensity from the ROE. This is particularly so for ROEs that involve NH protons resonating in the vicinity of side-chain amide and guanidino groups, which invariably give rise to large chemical exchange peaks with water.

In a series of recent papers we have presented the complete assignment of the backbone and side-chain $^1H$, $^{15}N$, and $^{13}C$ resonances of interleukin 1$\beta$, a protein of 153 residues and molecular mass of 17.4 kDa, together with an analysis of its secondary structure and molecular topology using a range of 3D double- and triple-resonance heteronuclear NMR experiments (Marion et al., 1989a; Driscoll et al., 1990a,b; Clore et al., 1990a). IL-1$\beta$ is itself of great interest as it is a member of the cytokine family of proteins, which play a central role in the immune and inflammatory responses [see Oppenheim et al. (1986), Dinarello (1988), and Moore (1989) for reviews]. Recently, two refined X-ray structures of IL-1$\beta$ at 2-Å resolution have been published (Finzel et al., 1989; Priestle et al., 1989), and a number of internal water molecules participating in stabilizing backbone interactions, particularly at the ends of $\beta$-sheets, have been identified (Finzel et al., 1989). In this paper, we make use of a novel 3D heteronuclear NMR experiment, 3D $^1H$ rotating-frame Overhauser $^1H$–$^{15}N$ multiple quantum coherence spectroscopy (ROESY-HMQC), to specifically identify NH protons in close proximity to bound water. By separating out the ROE and chemical exchange peaks into a third dimension on the basis of the $^{15}N$ chemical shift of nitrogens directly bonded to protons, the limitations of the 2D ROESY experiment are completely circumvented.

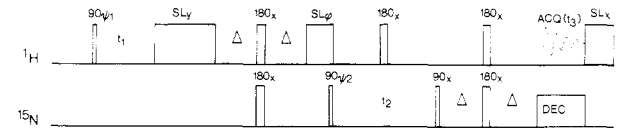


FIGURE 1: Pulse sequence for the $^1H$–$^{15}N$ ROESY-HMQC experiment. SL is a spin lock. ROESY mixing is achieved by a spin lock applied for 33 ms along the $y$ axis ($SL_y$). The two other spin-lock pulses ($SL_\phi$ and $SL_x$) are applied for only 2 ms. The delay $\Delta$ is set to 2.25 ms, slightly less than $1/(4J_{NH})$. $^{15}N$ decoupling during the acquisition period is achieved with WALTZ modulation (Shaka et al., 1983). The phase cycling is as follows: $\phi = 4(x), 4(-x)$ and Acq $= 2(x,-x,-x,x)$. Quadrature in $F_1$ and $F_2$ is obtained with the TPPI-States method (Marion et al., 1989b), using $\psi_1 = 4(x,-x)$, $4(y,-y)$ and $\psi_2 = 2(x,x,-x,-x)$, $2(y,y,-y,-y)$ and storing data for $\pm x$ and $\pm y$ components of $\psi_1$ and $\psi_2$ separately to be processed as complex data. Each time $t_1$ is incremented, $\psi_1$ and the receiver phase are increased by 180°, and similarly, each time $t_2$ is incremented, $\psi_2$ and the receiver phase are increased by 180°.

## Experimental Procedures

Uniformly labeled (>95%) [$^{15}N$]IL-1$\beta$ was prepared and purified as described previously (Wingfield et al., 1986; Driscoll et al., 1990a). Samples for NMR contained 2 mM [$^{15}N$]IL-1$\beta$ in 100 mM sodium acetate-$d_3$, pH 5.4, dissolved in 90% $H_2O$/10% $D_2O$. NMR spectra were recorded at 36 °C on a Bruker AM600 spectrometer, operating in the reverse mode. The 3D $^1H$–$^{15}N$ ROESY-HMQC spectrum was processed on a Sun Sparc station using an in-house routine for the $F_2$ Fourier transform, together with the commercially available 2D software package NMR2 (New Methods Research Inc., Syracuse, NY) for processing the $F_1$–$F_3$ planes, as described previously (Kay et al., 1989).

## Results and Discussion

The pulse scheme used for the 3D $^1H$–$^{15}N$ ROESY-HMQC experiment is given in Figure 1. After the evolution of $^1H$ chemical shifts during the period $t_1$, a 33-ms spin lock applied along the $y$ axis causes mixing of $^1H$ magnetization through chemical exchange and ROE effects (as well as some Hartmann–Hahn effects). At this stage, proton magnetization is aligned along the effective field, in the $yz$ plane, close to the $y$ axis. After dephasing caused by the $^{15}N$–$^1H$ $J$ coupling during the time period $2\Delta \sim 1/(2J_{NH})$, all magnetization residing on $^{15}N$-bound protons is subsequently converted into $^1H$–$^{15}N$ multiple quantum coherence by the application of a $^{15}N$ 90° pulse (Mueller, 1979). Note that magnetization from protons not attached to $^{15}N$, particularly $H_2O$ magnetization, remains aligned along the $y$ axis at the end of the interval $2\Delta$. The short 2-ms trim pulse applied along the $x$ axis then effectively removes this magnetization by randomization (Messerle et al., 1989), avoiding the necessity for presaturation of the $H_2O$ resonance. In this manner, water suppression is achieved without perturbing the observation of ROE effects between water and $^{15}N$-bound protons. During the evolution period $t_2$, $^1H$ offset effects are suppressed by the 180° $^1H$ pulse, and multiple quantum coherence evolves with the $^{15}N$ chemical shift frequency. At the end of the $t_2$ period, multiple quantum coherence is converted back to observable magnetization in the standard manner (Mueller, 1979; Bax et al., 1983). To ensure identical amounts of $z$ magnetization at the start of every sequence, a trim pulse is applied along the $x$ axis immediately after data acquisition. It is important to note that in this type of experiment the water magnetization is randomized and that recovery during the delay time between scans

[1] Abbreviations: IL-1$\beta$, interleukin 1$\beta$; NOE, nuclear Overhauser effect; ROE, rotating-frame Overhauser effect; 2D, two dimensional; 3D, three dimensional; $^{15}N$–$^1H$ ROESY-HMQC, three-dimensional $^1H$ rotating-frame Overhauser $^1H$–$^{15}N$ multiple quantum coherence spectroscopy.

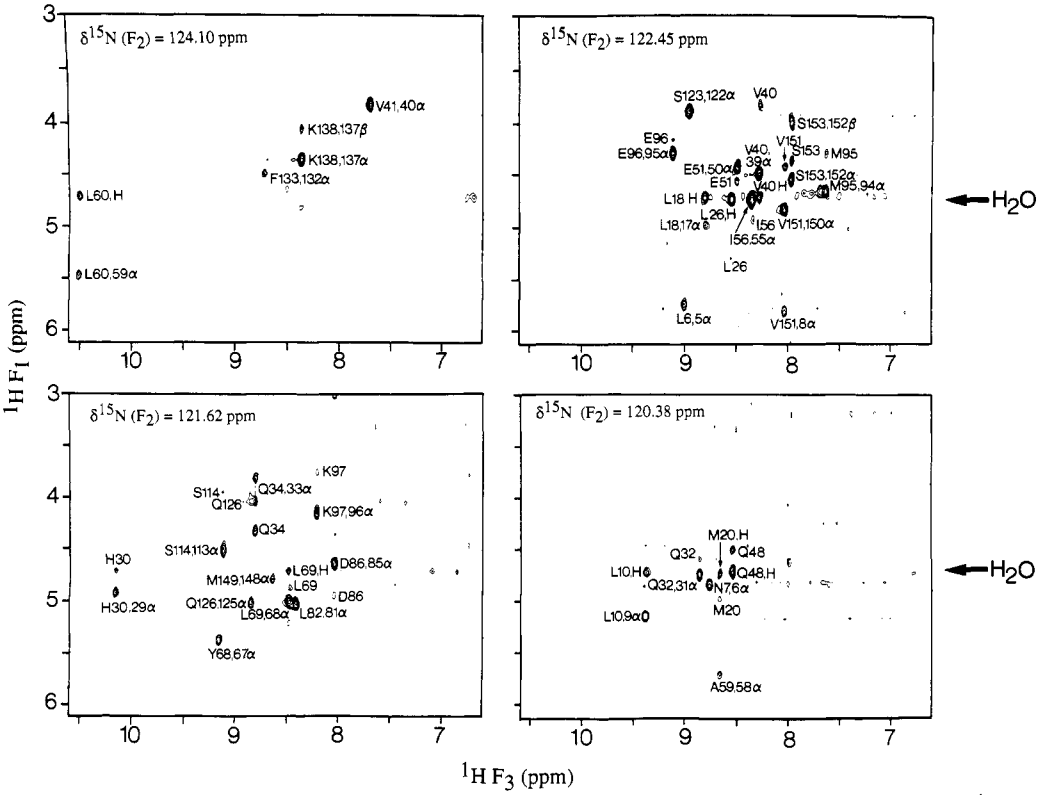


FIGURE 2: Four out of 64 ($F_1$,$F_3$) slices of the 3D $^1H$–$^{15}N$ ROESY-HMQC spectrum of 1.7 mM uniformly $^{15}N$-labeled IL-1$\beta$ in 90% $H_2O$ at pH 5.4 and 36 °C. Peaks are labeled *i,j*, where *i* refers to the NH proton (with the residue name and number indicated) and *j* refers either to water (indicated by the letter H) or to an aliphatic proton (indicated by the residue number and the proton type). The water frequency is at 4.67 ppm. The 3D spectrum results from a (128 complex) × (32 complex) × (512 real) data matrix, zero-filled to yield a final absorptive spectrum of 256 ($F_1$) × 64 ($F_2$) × 512 ($F_3$) data points. The total measuring time was ~48 h.

occurs with the longitudinal relaxation time $T_1$, which is often substantially longer than the $T_1$ of protein protons. In our particular case, using a delay time of 1.1 s between scans, protein protons have recovered ~65% of their equilibrium magnetization, whereas water protons have recovered only ~30% of their equilibrium value at the start of each scan. Thus, ROEs between water and protein protons are attenuated by a factor of about 2 relative to interactions among protein protons.

In the 3D spectrum each cross-peak is labeled by three chemical shifts: $^1H$ in $F_1$, $^{15}N$ in $F_2$, and $^{15}N$-bound $^1H$ in $F_3$. Each slice at a particular $^{15}N$ ($F_2$) frequency thus represents a 2D ROESY spectrum edited by $^{15}N$ chemical shifts.

The ROE mixing time (33 ms) was chosen to be about equal to the spin-locked relaxation time $T_{1\rho}$ of the amide protons, thus maximizing the signal-to-noise ratio of the ROE cross-peaks (Bothner-By et al., 1984; Bax & Davis, 1985). It is interesting to note that, even at this relatively long mixing period for a protein the size of IL-1$\beta$, the ROE intensities provide nearly quantitative distance information. For example, within the antiparallel $\beta$-sheets, the average sequential $C^\alpha H$-($i$)–NH($i$+1) ROE is about 6 times more intense than the average $C^\alpha H(i)$–NH($i$) ROE, in agreement with a factor of 5–7 predicted on the basis of a $r^{-6}$ dependence of the ROE intensity. As discussed previously (Bax et al., 1986), the good quantitative nature of the ROE intensity stems from the fact that the NOE under spin-locked conditions is positive, thereby strongly attenuating spin-diffusion effects.

Cross-peaks in the $^1H$–$^{15}N$ ROESY-HMQC spectrum may arise from one of three sources. Negative cross-peaks (of opposite sign to the diagonal peaks at $\delta F_1 = \delta F_3$) arise from NOEs in the rotating frame, known as ROEs. Chemical exchange, on the other hand, gives rise to positive cross-peaks. Hartmann–Hahn effects may also give rise to positive cross-peaks but will only be evident when the matching for homonuclear Hartmann–Hahn transfer is near perfect, that is to say when the two $^1H$ spins have opposite but approximately equal offsets from the transmitter (Bax, 1988). In considering the origin of negative cross-peaks between NH protons and water, two possible mechanisms must be considered. The first involves solely an ROE and is due to the close proximity of the NH proton and the bound water molecule. The second involves an indirect pathway whereby magnetization is transferred between an NH proton and a rapidly exchanging side-chain proton (i.e., hydroxyl group in Ser, Thr, and Tyr, the side-chain amide group in Asn, Gln, and Lys, and the guanidinium group in Arg), followed by chemical exchange between the latter proton and water. Providing the three-dimensional structure of the protein under consideration is known, the possible contribution of the latter magnetization-transfer pathway can be readily assessed.

Four slices at different $^{15}N$ chemical shifts of the 3D $^1H$–$^{15}N$ ROESY-HMQC spectrum are shown in Figure 2, and it can be clearly seen that there are a number of ROE cross-peaks between NH protons in the $F_3$ dimension and the water resonance frequency in the $F_1$ dimension. These cross-peaks involve Leu-60 NH at $\delta^{15}N$ = 124.10 ppm, Leu-18 NH, Leu-26 NH, and Val-40 NH at $\delta^{15}N$ = 122.45 ppm, Leu-69 NH at $\delta^{15}N$ = 121.62 ppm, and Leu-10 NH and Met-20 NH at $\delta^{15}N$ = 120.38 ppm. We were able to identify 17 such cross-peaks in the complete 3D data set, which could not be attributed to ROEs between NH protons and $C^\alpha H$ protons degenerate with the water resonance. (An example of the latter is the cross-peak seen in Figure 2 between Ile-56 NH and Lys-55 $C^\alpha H$ at $\delta^{15}N$ = 122.45 ppm.) The residues corresponding to these 17 cross-peaks are Leu-10, Leu-18,

Met-20, Leu-26, Ala-28, Leu-31, Val-40, Gln-48, Glu-50, Leu-60, Leu-69, Phe-112, Ala-115, Gln-116, Ser-125, Asn-129, and Met-130. Examination of the crystal structure of IL-1$\beta$ (Finzel et al., 1989) indicates that for 15 of these 17 NH protons there are no labile side-chain protons in close proximity (i.e., <3.5 Å) so that these effects can be attributed directly to ROEs involving bound water. In the case of Ala-115 and Gln-116, however, the NH protons are ~2.5 Å away from the hydroxyl group of Ser-114 so that an alternative pathway involving an ROE to the O$^{\gamma}$H of Ser-114 followed by chemical exchange of the hydroxyl proton with water is possible.

The intensity of a cross-peak between an NH proton and bound water depends both on the proximity of the NH proton to the water protons and on the lifetime of the bound water molecule. A rough estimate on the lower limit of the bound water lifetime, however, can be obtained as follows. The intensities of the ROE cross-peaks with bound water vary from 3 to 8 times lower than the average intensity of the C$^{\alpha}$H($i$)–NH($i$+1) sequential ROE peaks within a $\beta$-sheet, which corresponds to a distance of ~2.2 Å. As discussed above, the ratios of ROE cross-peak intensities at the mixing time (33 ms) employed still provide a good estimate of interproton distance ratios. Hence, the intensity of a ROESY peak between two protons is a direct reflection of the corresponding dipole–dipole relaxation rate in the rotating frame. This rate is in turn directly proportional to the inverse sixth power of the distance and $f(\tau_{eff}) = 4\tau_{eff} + 6\tau_{eff}/(1 + \omega^2\tau_{eff}^2)$, where $\tau_{eff}$ is the effective correlation time of the interproton vector and $\omega$ the spectrometer frequency. Ignoring internal motion, $\tau_{eff}$ is given approximately by $\tau_{eff}^{-1} \sim \tau_R^{-1} + \tau_{ex}^{-1}$, where $\tau_R$ and $\tau_{ex}$ are the rotational correlation time of the protein and the lifetime of the bound water molecule, respectively. If the residence time of the bound water molecule is much longer than $\tau_R$, the ROE intensity, for a given interproton distance, is determined solely by the overall tumbling time of the protein, which in this case is 8.3 ns (Clore et al., 1990b). If, on the other hand, the lifetime $\tau_{ex}$ is much shorter than $\tau_R$, the ROE will be determined by $\tau_{ex}$. If we assume that we could detect a cross-peak up to 20 times less intense than the sequential C$^{\alpha}$H($i$)–NH($i$+1) cross peaks within an antiparallel $\beta$-sheet, then an ROE between an NH proton ~2, ~2.5, and ~3 Å away from a water proton (taking into account the 2-fold attenuation of ROEs involving water protons relative to those involving only protein protons, mentioned above) could still be observed at a mixing time of ~30 ms providing the lifetime of the bound water molecule would be greater than about 0.2, 2, and 8 ns, respectively.

Because the bound water resonances are degenerate with water, it is clear that the results can only be interpreted in structural terms in light of a high-resolution structure of IL-1$\beta$. Examination of the X-ray structure of IL-1$\beta$ reveals the presence of 84 bound water molecules (Finzel et al., 1989). We, however, only observe ROEs involving a small proportion of these, and in each case, the water molecule involved takes part in bridging backbone hydrogen bonds of the type NH---OH---CO. In the case of 12 of the 15 NH protons, the NH proton is itself hydrogen bonded to water, whereas in the other three cases (Val-40, Leu-69, and Asn-129) it is within close proximity (<3 Å) of a bound water molecule. These interactions are summarized in Figure 3.

The overall topology of IL-1$\beta$ displays internal pseudo-3-fold symmetry (Priestle et al., 1988; Finzel et al., 1989; Driscoll et al., 1990b). Each topological unit is composed of five antiparallel $\beta$-strands (Figure 3A–C), which we shall denote as A–E. These form three antiparallel $\beta$-sheets in a triangular

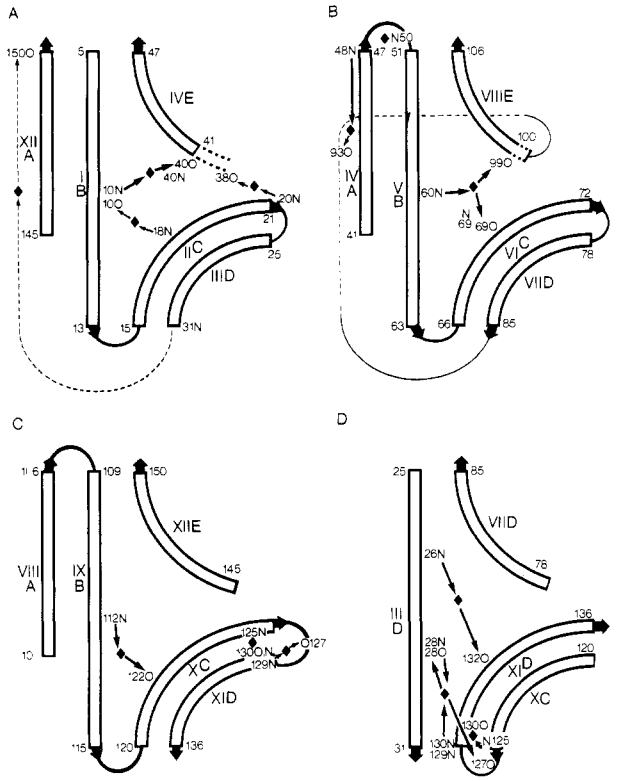


FIGURE 3: Location of bound water molecules in IL-1$\beta$ deduced from the presence of ROESY cross-peaks between NH protons and water in the 3D $^1$H–$^{15}$N ROESY-HMQC experiment. The molecular topology of IL-1$\beta$, derived from both NMR (Driscoll et al., 1990b) and crystallographic (Finzel et al., 1989) data, is depicted schematically. The three repeating topological units, each composed of five antiparallel $\beta$-strands, are shown in (A)–(C), and the interface of the three units is shown in (D). The NH protons that are involved in ROESY cross-peaks with water are indicated by residue name and number, and the water molecules are depicted as diamonds. The hydrogen-bonding interactions of these water molecules, as seen in the crystal structure, are indicated by the arrows.

arrangement. Thus, one sheet is formed by strands A and B and the C-terminal end of E, another comprises strands D and C and the C-terminal end of strand B, while the third is made up from strands C and D and the N-terminal end of strand E. Strands B and C are connected by a tight turn, while strands C and D are connected by either a turn or a longer loop. There are a total of 12 $\beta$-strands (I–XII), and strand A is equivalent to strands XII (Figure 3A), IV (Figure 2B), and VIII (Figure 3C) in the first, second, and third topological unit, respectively, strand B to strands I, V, and IX, strand C to strands II, VI, and X, strand D to strands III, VII, and XI, and finally strand E to strands IV, VIII, and XII. Note that strand XII is strand A in the first unit and strand E in the third, strand IV is strand A in the second unit and strand E in the first, and strand VIII is strand A in the third unit and strand E in the second. The three units are linked together by three antiparallel $\beta$-sheets formed by the D strands of each topological unit (Figure 3D).

Three of the internal molecules that we observe occur in approximately the same location, although not necessarily in the same orientation, within each of the three topological units and form a bridge between strands B and C (Figure 3A–C). Thus, a water molecule bridges Leu-18 NH (strand II/C) and Leu-10 CO (strand I/B) in the first unit (Figure 3A), Leu-60 NH (strand V/B) and Leu-69 CO (strand VI/C) in the second unit (Figure 3B) with the NH of Leu-69 in close proximity to the water molecule, and Phe-112 NH (strand XI/B) and Ile-122 CO (strand X/C) in the third unit (Figure 3C). The

fact that the NH protons of Leu-18 and Leu-60 are directly hydrogen bonded to a water molecule, while that of Leu-69, albeit in close vicinity to a bound water molecule, is not, is borne out by the significantly lower intensity of the Leu-69–$H_2O$ cross-peak compared to that of the other two cross-peaks (see Figure 2). The linkage between two of the D strands, strand III and XI, formed by a bridging water between Leu-26 NH and Val-132 CO, is also located in an approximately topologically equivalent position to that of the above three water molecules (Figure 3D). In the case of the first and second units, we also observe a water molecule bridging strands B and E. Thus, in the first unit there is a water bridging Leu-10 NH (strand IB) and Val-40 CO with the NH of Val-40 in close proximity to the bound water. In the second unit, the same water molecule that serves to bridge strands B and C also bridges strands B and E via Leu-60 NH---OH---Phe-99 CO hydrogen bonds. In the crystal structure there is also a water molecule that bridges strands E and C between Thr-144 NH (strand XII/E) and Ile-122 CO. However, no ROESY cross-peak is observed between the NH of Thr-144 and the water resonance.

In addition to the five water molecules discussed above, the NMR data indicate the presence of another six bound waters. Three of these occur in turns. In particular, there is one bound water in the turn connecting strands IV and V (Figue 3B) with a hydrogen bond formed between Glu-50 NH and a water molecule, and there are two bound waters in the turn joining strands X and XI bridging Ser-125 with Met-130 and Asn-129 with Ala-127 (Figure 3C,D). The latter also serves as a connection between that turn and strand III (Figure 3D). Three structural water molecules are involved in bridging ends of $\beta$-strands that are not linked together in an antiparallel $\beta$-sheet. These connections serve to close the approximately tetrahedral molecule at the corners and comprise Leu-31 NH---OH---Phe-150 CO hydrogen bonds bridging strands III/C and XII/A, while strands II/C and IV/E are joined via the Met-20 NH---OH---Gln-38 CO hydrogen-bonding network. Likewise, strand IV/E and the loop at the C-terminal end of strand VII/C are connected via the Gln-48 NH---OH---Lys-93 CO hydrogen bonds (Figure 3B).

## Concluding Remarks

In this paper we have directly demonstrated the presence of a number of bound water molecules in IL-1$\beta$ which are in close proximity to backbone amide protons, by means of a 3D $^1H$–$^{15}N$ ROESY-HMQC experiment. These could be attributed to 11 water molecules out of the total of 84 observed in the crystal structure. All the water molecules that we observe are involved in interactions with backbone groups that stabilize the structure of the protein and thus constitute an integral part of the protein structure in solution. Given a minimum interproton distance separation of $\sim$2 Å between an NH proton and a water proton, we can deduce that the shortest lifetime for a bound water molecule consistent with the observation of an ROE peak at a short mixing time ($\sim$30 ms) is about 0.2 ns. For longer distances, this value goes up significantly such that at 2.5 Å the minimum lifetime is $\sim$2 ns and at 3 Å it is $\sim$8 ns. There are 27 water molecules in the crystal structure whose protons are within 2.5 Å of an NH proton. Of these, we only observe ROEs involving 11 of them, so that the remaining 17 must exchange rather rapidly in solution, possessing lifetimes shorter than about 2 ns.

## Acknowledgments

We thank Dr. Barry Finzel for providing us with the X-ray coordinates of IL-1$\beta$.

**Registry No.** $H_2O$, 7732-18-5.

## References

Baker, E., & Hubbard, R. (1984) *Prog. Biophys. Mol. Biol. 44*, 97.

Bax, A. (1988) *J. Magn. Reson. 77*, 134–147.

Bax, A., & Davis, D. G. (1985) *J. Magn. Reson. 63*, 207–213.

Bax, A., Griffey, R. H., & Hawkins, B. L. (1983) *J. Magn. Reson. 55*, 301–315.

Bax, A., Sklenar, V., & Summers, M. F. (1986) *J. Magn. Reson. 70*, 327–331.

Bode, W., & Schwager, P. (1975) *J. Mol. Biol. 98*, 139–143.

Bothner-By, A. A., Stephens, R. L., Lee, J. T., Warren, C. D., & Jeanloz, R. W. (1984) *J. Am. Chem. Soc. 106*, 811–813.

Brändén, C. I., Jornvall, H., Eklund, H., & Furugren, B. (1975) *Enzymes (3rd Ed.) 3*, 103–190.

Brünger, A. T., Brooks, C. L., & Karplus, M. (1985) *Proc. Natl. Acad. Sci. U.S.A. 82*, 8458–8462.

Carter, C. W., Kraut, J., Freer, S. T., & Alden, R. A. (1974) *J. Biol. Chem. 249*, 4212–4225.

Clore, G. M., Bax, A., Driscoll, P. C., Wingfield, P. T., & Gronenborn, A. M. (1990a) *Biochemistry* (submitted for publication).

Clore, G. M., Driscoll, P. C., Wingfield, P. T., & Gronenborn, A. M. (1990b) *Biochemistry* (in press).

Davis, D. G., & Bax, A. (1985) *J. Magn. Reson. 64*, 533–535.

Deisenhofer, J., & Steigemann, W. (1975) *Acta Crystallogr., Sect. B 31*, 238–250.

Dinarello, C. A. (1984) *Ann. N.Y. Acad. Sci. 546*, 122–132.

Driscoll, P. C., Clore, G. M., Marion, D., Wingfield, P. T., & Gronenborn, A. M. (1990a) *Biochemistry 29*, 3542–3556.

Driscoll, P. C., Gronenborn, A. M., Wingfield, P. T., & Clore, G. M. (1990b) *Biochemistry 29*, 4668–4682.

Edsall, J. T., & McKenzie, H. A. (1983) *Adv. Biophys. 16*, 53–183.

Finney, J. L. (1979) in *Water: A Comprehensive Treatise* (Franks, F., Ed.) Vol. 6, pp 47–123, Plenum Press, New York.

Finzel, B. C., Clancy, L. L., Holland, D. R., Muchmore, S. W., Watenpaugh, K. D., & Einspahr, H. M. (1989) *J. Mol. Biol. 209*, 779–791.

Halle, B., Anderson, T., Forsén, S., & Lindman, B. (1981) *J. Am. Chem. Soc. 103*, 500–508.

James, M. N. G., & Sielecki, A. R. (1983) *J. Mol. Biol. 163*, 299–361.

Jeener, J., Meier, B. H., Bachman, P., & Ernst, R. R. (1979) *J. Chem. Phys. 71*, 4546–4553.

Kay, L. E., Marion, D., & Bax, A. (1989) *J. Magn. Reson. 84*, 72–84.

Koenig, S. H., Bryant, R. G., Hallenga, K., & Jacob, G. S. (1978) *Biochemistry 17*, 4348–4358.

Marion, D., Driscoll, P. C., Kay, L. E., Wingfield, P. T., Bax, A., Gronenborn, A. M., & Clore, G. M. (1989a) *Biochemistry 28*, 6150–6156.

Marion, D., Ikura, M., Tschudin, R., & Bax, A. (1989b) *J. Magn. Reson. 85*, 393–399.

Messerle, B. A., Wider, G., Otting, G., Weber, C., & Wüthrich, K. (1989) *J. Magn. Reson. 85*, 608–613.

Moore, M. A. S. (1989) *Immunol. Res. 8*, 165–175.

Mueller, L. (1979) *J. Am. Chem. Soc. 101*, 4481-4484.
Oppenheim, J. J., Kovacs, E. J., Matsushima, K., & Durum, S. K. (1986) *Immunol. Today 7*, 45-56.
Otting, G., & Wüthrich, K. (1989) *J. Am. Chem. Soc. 111*, 1871-1875.
Priestle, J. P., Schär, H. P., & Grütter, M. G. (1988) *EMBO J. 7*, 339-343.
Priestle, J. P., Schär, H. P., & Grütter, M. G. (1989) *Proc. Natl. Acad. Sci. U.S.A. 86*, 9667-9671.
Redfield, A. G. (1983) *Chem. Phys. Lett. 96*, 537-540.
Rees, D. C., Lewis, M., & Lipscomb, W. N. (1983) *J. Mol. Biol. 168*, 367-387.
Rose, G. D. (1978) *Nature (London) 272*, 586-590.
Shaka, A. J., Keeler, J., Frenkiel, T., & Freeman, R. (1983) *J. Magn. Reson. 52*, 335-338.
Shirley, W. M., & Braynt, R. G. (1982) *J. Am. Chem. Soc. 104*, 2910-2918.
Teeter, M. (1984) *Proc. Natl. Acad. Sci. U.S.A. 81*, 6014-6018.
Tüchsen, T., Hayes, J. M., Ramaprasad, S., Copie, V., & Woodward, C. (1987) *Biochemistry 26*, 5163-5172.
Wingfield, P. T., Payton, M., Tavernier, J., Barnes, M., Shaw, A., Rose, K., Simona, M. G., Demaczuk, S., Williamson, S., & Dayerm, J.-M. (1986) *Eur. J. Biochem. 160*, 491-497.
Wlodawer, A., Deisenhofer, J., & Huber, R. (1987) *J. Mol. Biol. 193*, 145-156.

## *Articles*

# DNA Strand Scission by the Novel Antitumor Antibiotic Leinamycin

Mitsunobu Hara,* Yutaka Saitoh, and Hirofumi Nakano
*Tokyo Research Laboratories, Kyowa Hakko Kogyo Ltd, Asahi-machi 3-6-6, Machida-shi, Tokyo, Japan*
*Received October 20, 1989; Revised Manuscript Received March 7, 1990*

ABSTRACT: Leinamycin is a recently discovered antitumor antibiotic with an unusual 1,3-dioxo-1,2-dithiolane structure. It preferentially inhibits the incorporation of [$^3$H]thymidine into the acid-insoluble fraction of *Bacillus subtilis*. In vitro, leinamycin causes single-strand cleavage of supercoiled double-helical pBR322 DNA in the presence of thiol cofactors. Scavengers of oxygen radical did not supress the DNA-cleaving activity. Thiol-activated leinamycin binds calf thymus DNA at 4 °C and thermal treatment of the leinamycin–DNA adduct released a chemically modified leinamycin from the complex. The lack of cytotoxicity and DNA-cleaving activity for *S*-deoxyleinamycin indicates that the 1,3-dioxo-1,2-dithiolane moiety is essential for the activity of leinamycin. Thus, the primary cellular target of leinamycin appears to be DNA. It binds DNA and causes single-strand break at low concentrations, which may account for the potent antitumor activity.

DNA is thought to be the principal target of a number of clinically useful antitumor agents including, mitomycin, bleomycin, adriamycin, and *cis*-platinum. These compounds interfere with DNA through cross-linkage, strand breakage, intercalation, or other kinds of interactions, which result in inhibition of nucleic acid synthesis (Tomasz et al., 1987; Stubbe & Kozarich, 1987; Rowley & Halliwell, 1983; Eastman, 1985). The discovery of these antitumor agents which interact with DNA has provided insight into the mechanistic principle that can be used to mediate DNA recognition and cleavage.

In the course of screening for antitumor antibiotics, we have isolated a new antitumor antibiotic, leinamycin, produced by a *Streptomyces* sp. (Hara et al., 1989a,b). The structure of leinamycin (Figure 1) was revealed by X-ray crystallography and the absolute configuration of the antibiotic was determined by spectroscopic and chemical analysis (Hirayama & Shimizu, 1989; Saitoh et al., 1989). Leinamycin contains an unusual 1,3-dioxo-1,2-dithiolane moiety, which is connected to the 18-membered lactam ring through a spiro linkage, and can be classified as a new group distinct from any known classes of antibiotics or microbial metabolites. Leinamycin exhibited potent antitumor activity against murine experimental tumors leukemia P388 and sarcoma 180. The compound was also active against Gram-positive bacteria (Hara et al., 1989a). The unique structural features as well as the high biological activity of leinamycin prompted us to investigate the mode of action of this antitumor agent. We report here the effect of leinamycin on bacterial DNA synthesis, binding, and single-strand scission of DNA in vitro through the thiol-activated 1,3-dioxo-1,2-dithiolane moiety.

## Materials and Methods

*Chemicals and Enzymes.* Leinamycin was isolated from a cultured broth of *Streptomyces* sp. as reported previously (Hara et al., 1989a,b). Stock solutions were prepared in DMSO and stored at −20 °C. [6-$^3$H]Thymidine (15Ci/mmol), [2-$^{14}$C]uracil (57.4mCi/mmol), [4,5-$^3$H]leucine (5Ci/mmol), and [$\gamma$-$^{32}$P]ATP (10Ci/mmol) were purchased from New England Nuclear, Boston, MA. All other reagents used were of commercial reagent grade.

*Preparation of S-Deoxyleinamycin.* The *S*-deoxy derivative was prepared by hydrogenolysis of leinamycin in the presence of 5% Pd–C in methanol. Details of this compound will be discussed elsewhere (Saitoh et al., 1989).

*Effect of Leinamycin on the Growth and Macromolecular Synthesis of Bacillus subtilis. B. subtilis* was cultured in medium containing 0.2 g of $MgSO_4 \cdot 7H_2O$, 2 g of citric acid (10 g of $KH_2PO_4$, 3.5 g of $NaNH_4HPO_4 \cdot H_2O$, 5 g of glucose, 1 g of casamino acids, 2 g of yeast extract, 50 mg of tryptophan, and 50 mg of arginine per liter of deionized water (pH 7.0). Various amounts of leinamycin were added at 1.7 h, and

0006-2960/90/0429-5676$02.50/0 